

OASIS98 Radiometer Report

1999 April 19 version, incorporating TH's and SR's simple corrections. Substantive corrections yet to be addressed.

The responses of the radiometers deployed for the OASIS98 program were compared. The NCAR and the OKMN four component arrays both consisted of sets of Eppley radiometers, an upward and a downward looking pyrgeometer and an upward and a downward looking pyranometer. The CNR1 was an integrated sensor manufactured by Kipp and Zonen. The NCAR four-component Eppley array was fully ventilated, the OKMN four-component Eppley array had ventilation only for the upward-looking radiometers and the two integrated four-component CNR1 instruments were not heated but were ventilated. Two REBS Q7 net radiometers were deployed, one with the NCAR array and one with the OKMN array. Seven NRLite, Kipp and Zonen net radiometers were deployed with the OKMN array. The NCAR sensors were supported at the middle of a 3m long east-west beam 2m above the surface and the OKMN sensors were supported by an east-west beam 3m above the surface.

The ASTER data system acquired and processed the output from the sensors and was used to generate the graphical product for intercomparisons.

Treatment of the NCAR four-component Eppley array data

Values for Rsw.in/out were determined from the output of the array taken with the manufacturer's calibration factors.

Values for Rlw.in/out, were calculated from output of the array taken with the calibration factors using equation (1). Prior to the calculations the specification, Robust=F was made to ensure that the dome/case and the visible sensitivity correction terms were utilized.

$$Rlw = Rpile + (1 + B) * SB * Tcase^4 - B * SB * Tdome^4 - 0.035 Rsw \quad (1)$$

Equation (1) is equivalent to the basic expression (2) which shows the separate factors.

$$Rlw = Rpile + [SB * (Tcase)^4] - [B * SB * ((Tdome)^4 - (Tcase)^4)] - [0.035 * Rsw] \quad (2)$$

where: SB is the Stefan Boltzman constant = $5.67 * 10^{-8}$, when T is in degreeK and the output is in Wm^{-2} .

B, the dome opaqueness coefficient, is settable but 2.5 by default.

Rlw.in, Rlw.out, Rsw.in and Rsw.out were then algebraically summed to yield Rsum.

Tsky and Tsvc were calculated from the Rlw.in/out.

Treatment of the OKMN four-component Eppley array data

Calibrated values for Rsw.in/out from the OKMN Eppley four component array were input to ASTER and were utilized. However, although the Rlw.in/out parameters were also accepted, Rlw.in/out were recalculated using the NCAR algorithms for equation (1), with Robust=F, to ensure that the values were generated in the same manner as were the NCAR Rlw.in/out.

Rlw.in, Rlw.out, Rsw.in and Rsw.out were then algebraically summed to yield Rsum

Treatment of the OKMN integrated CNR1 four-component sensor data

The CNR1 integrated four-component sensor apparently contains a microprocessor. This microprocessor yields calibrated values of Rsw.in/out, Rpile.in/out, Tcase and of Rlw.in/out and Rnet (Rsum).

As the CNR1 integrated four-component radiometer does not have pyrgeometer dome temperature measurement capability, Rlw.in/out could not be corrected for the effect of dome heating. Whether or not a short-wave sensitivity correction is needed is unknown. The CNR1 was not ventilated but a 1 Watt heater was operated continuously to keep the domes dew-free. This could potentially cause a temperature offset. The CNR1 integrated sensor values for Rsw.in/out, Rlw.in/out and Rnet (Rsum) were passed via the OKMN data system directly to the ASTER data system. These were the values utilized in the comparison.

TABLE 1 Oasis98 Radiation parameters used in comparisons

NCAR		OKMN		OKMN (extra)	
4-comp Eppley, full vent'd		4-comp Eppley, top only vent'd		<p>The comparison of CNR1a and CNR1b, and of NRLite1 with NRLite2-7 has already been carried out by OKMN people. They are satisfied as to the consistency of the sensor sets.</p>	
Rsw.in	NCAR data	Rsw.in	OK data		
Rsw.out		Rsw.out			
Tdome.in		Tdome.in			
Tdome.out		Tdome.out			
Tcase.in		Tcase.in			
Tcase.out		Tcase.out			
Rpile.in		Rpile.in			
Rpile.out		Rpile.out			
Rlw.in	Rlw calculated	Rlw.in	OK data supplied but Rlw recalculated from OK data using NCAR algorithms. Robust = F		
Rlw.out	When Robust = F Dome/case and Visible light corrections made	Rlw.out			
Rsum		Rsum			
Tsky	Calculated from Rlw.in, Rlw.out	Tsfc	Calculated from Rlw.in, Rlw.out		
Tsfc		Tsky			
		CNR1a, unventilated		CNR1b, unventilated	
		Rsw.in.CNR1a	K&Z output data supplied via OK	Rsw.in.CNR1b	OK data available but not used
		Rsw.out.CNR1a		Rsw.out.CNR1b	
		Rpile.in.CNR1a		Rpile.in.CNR1b	
		Rpile.out.CNR1a		Rpile.out.CNR1b	
		Tcase.in.CNR1a		Tcase.out.CNR1b	
		Rlw.in.CNR1a		Rlw.in.CNR1b	
		Rlw.out.CNR1a		Rlw.out.CNR1b	
Rnet.CNR1a, (Rsum.CNR1a)	Rnet.CNR1a, (Rsum.CNR1b)				
Q7		Q7			
Rnet	NCAR data	Rnet	OK data		
		NRLite.1		NRLite.2	
		Rnet.NRLite1	OK data	Rnet.NRLite2	Avbl,not usd
				NRLite.3	
		Rnet.NRLite3	Avbl,not usd		
				NRLite.4	
		Rnet.NRLite4	Avbl,not usd		
				NRLite.5	
		Rnet.NRLite5	Avbl,not usd		
				NRLite6	
		Rnet.NRLite6	Avbl,not usd		
		NRLite7			
Rnet.NRLite7	Avbl,not usd				

Comparison of radiometer response

A comparison of the radiometers' response for a cloudless day was performed. Inspection of the radiation record from the beginning of the program until July 20, indicates that July 15 was a nearly perfect day. The 24 hour period; July 14, 18:00 until July 15, 18:00 was used to compare radiometer responses. The most cloudy day of the OASIS98 deployment was 4 Aug. An analysis of this cloudy day was performed following the same procedure as for the 14 July best day. The nature of the cloudiness, however was not good from a radiation point of view (a uniform total overcast would have been desirable), and not much new information was derived. Due to the prolonged heat-wave there was no opportunity to carry out a comparison of the responses of the radiometers for a diffuse radiation, overcast day. At the end of the deployment the eight Eppley radiometers were all mounted to face upward to the sky. This change was made in the late afternoon, Friday, 7 Aug, and the radiometers remained in this configuration until mid-morning, Sunday, 9 Aug. The morning of Saturday, 8 Aug was cloudy with some rain, but just before noon the sky cleared and for the rest of the period there were no clouds.

The three four components system each yield their individual four components Rsw.in, Rsw.out, Rlw.in and Rlw.out, as well as their algebraically added summation or "Rsum". The net radiometers each yield a single value of the net total radiation

Incoming short-wave radiation

NCAR and OKMN agree well during the day, with a maximum difference

$$\text{OKMN}_{\text{sw.in}} < \text{NCAR}_{\text{sw.in}} \text{ by } 20 \text{ Wm}^{-2} \text{ at noon.}$$

The CNR1a shows a greater difference with a maximum difference

$$\text{CNR1}_{\text{asw.in}} < \text{NCAR}_{\text{sw.in}} \text{ by } 60 \text{ Wm}^{-2} \text{ at noon}$$

At night the $\text{OKMN}_{\text{sw.in}}$ is set, by software, to be 0.0 Wm^{-2} . The $\text{NCAR}_{\text{sw.in}}$ has an instrumentation response of -4 to -2 Wm^{-2} . The $\text{CNR1}_{\text{asw.in}}$ also shows this instrumentation response. For the CNR1a the value is -10 Wm^{-2} .

TABLE 2 Incoming short-wave radiation

Radiometer	Night-time	Daytime
NCAR _{sw.in}	Instrumentation response of -4 to -2 Wm^{-2}	NCAR _{sw.in} ~ OKMN _{sw.in} OKMN _{sw.in} < NCAR _{sw.in} by 20 Wm^{-2} at noon. CNR1 _{asw.in} < NCAR _{sw.in} by 60 Wm^{-2} at noon
OKMN _{sw.in}	Set to 0.0 Wm^{-2}	
CNR1 _{asw.in}	Instrumentation response of -10 Wm^{-2}	

These nighttime negative instrumentation responses are due to a real export of energy by the radiometers. The treatment of the OKMN sw data is probably reasonable, but masks the problem of instrument response, which also occurs during the daytime.

Outgoing short-wave radiation

In the day time the three systems differ over a range of 25 Wm^{-2} at noon. As the three look down at different surfaces this can be due to the albedo differences. Thus the OKMN albedo may be greater than that for the NCAR site because a different grass cutting method is used for the land under the OKMN radiometer stands.

TABLE 3 Outgoing short-wave radiation

Radiometer	Night-time	Daytime
NCAR _{sw.out}	Instrumentation response of -2 Wm^{-2}	Total range 25 Wm^{-2} Much of this difference may be due to different surface albedos
OKMN _{sw.out}	Set to 0.0 Wm^{-2}	
CNR1 _{asw.out}	Instrumentation response of -5 Wm^{-2}	

There is also more surface shading directly under the radiometers on the NCAR stand by the CR10 box, boom and four-component mount. However, the calculation presented in the Appendix, indicates that the influence of the shadows present is inconsequential, even at solar noon when the effect is $\sim 2\%$.

Incoming long-wave radiation

The OKMN_{lw.in} response is very similar to the NCAR_{lw.in} response, both in the day and at night, with the exception of the 15 Wm^{-2} higher value for the 3 hour period around noon. This anomaly may be due to photodegradation of the vacuum-deposited silicon coating on the pyrgeometer dome.

At night the CNR1_{alw.in} shows a fairly consistent offset with $\text{CNR1alw.in} > \text{NCARlw.in}$ by 20 to 30 Wm^{-2}

TABLE 4 Incoming long-wave radiation

Radiometer	Night-time	Daytime
NCAR _{lw.in}	NCAR \sim OKMN	$+15 \text{ Wm}^{-2}$ anomaly at midday
OKMN _{lw.in}		
CNR1 _{alw.in}	$\text{CNR1a} > \text{NCAR}$ by 20 to 30 Wm^{-2}	$\text{CNR1a} > \text{NCAR}$ increase to 60 Wm^{-2}

In the daytime $\text{CNR1alw} > \text{NCARlw}$ increases with a maximum difference of $+60 \text{ Wm}^{-2}$ at midday. This could be due to an incomplete dome heating correction or even to sensitivity to sw radiation.

Outgoing long-wave radiation

The response of the three radiometer to the emission of lw radiation by the surface is simple.

OKMN_{lw.out} $<$ NCAR_{lw.out} by 5 Wm^{-2} at night,
 OKMN_{lw.out} $>$ NCAR_{lw.out} by 5 Wm^{-2} by day

Similarly

CNR1_{alw.out} $>$ NCAR_{lw.out} by 20 Wm^{-2} by night
 CNR1_{alw.out} $>$ NCAR_{lw.out} by 35 Wm^{-2} by day

TABLE 5 Outgoing long-wave radiation

Radiometer	Night-time	Daytime
NCARlw.out		
OKMNIw.out	OKMN < NCAR by 5 Wm ⁻²	OKMN < NCAR by 5 Wm ⁻²
CNR1alw.out	CNR1a > NCAR by 20 Wm ⁻²	CNR1a > NCAR by 235 Wm ⁻²

The difference of both the OKMNIw.in and the OKMNIw.out to the NCARlw appear to be offsets rather than proportional differences in gain.

Net radiation

The convention employed in this discussion is that “*sum” parameters are generated from the algebraic addition of the four components while the “*net” parameters correspond to the output of integral net radiometers. Note that although the K&Z four component output is designated "Rnet.CNR1a", it is a summation product, and here is termed CNR1asum.

The general agreement was good with the most significant disagreements being the OKMNQ7 at night and the NRLite at noon. The midday anomaly of the OKMNIw is obvious.

The response of the six net radiation systems are all within a range of ~20-40 Wm⁻² varying from ~ -40 - 60 throughout the nighttime

TABLE 6 Responses of the sum/net systems compared to the NCARsum:

Radiometer	Night-time	Noon
OKMNsum	+10 Wm ⁻²	-25 Wm ⁻² if noon anomaly removed
NCARQ7	+10 Wm ⁻²	-15 Wm ⁻²
OKMNQ7	+25 Wm ⁻²	-20 Wm ⁻²
CNR1asum:	+0 Wm ⁻²	-30 Wm ⁻²
NRLite:	+15 Wm ⁻²	-50 Wm ⁻²

Conclusions

An absolute standard for intercomparison is difficult to define, inasmuch as both the Eppley and the Kipp and Zonen have their supporters in the atmospheric radiation community. However, the thermopile response of all four radiometers making up the NCAR four component array have recently (immediately prior to OASIS98) been individually calibrated by the NOAA Atmospheric Radiation Group, in Boulder, and the dome and case thermister response have been characterized in the SSSF calibration lab. In addition, we have several year's experience with this array as part of the ASTER sensor system and during OASIS we ensured that the radiometer array was level, the domes were clean, the ventilation was maintained and the surface below the array was undisturbed. On the other hand the CNR1 is not the top-of-the-line Kipp and Zonen sensor. These considerations give more credibility to the NCAR four component system.

Surface albedo. The radiometers were not situated over identical surfaces. Particularly for the outgoing short-wave radiation, this difference in albedo caused a significant true difference in response. Comparison of the NCAR and the OKMN pyranometers output suggests that this factor accounts for $\sim 15 \text{ Wm}^{-2}$ difference in the contribution, at noon, of the outgoing short-wave radiation to the net flux. There is, however, the issue of some corresponding compensation in the long-wave due to the lesser heating effect when more short wave radiation is reflected rather than absorbed. The difference of the two surfaces could be perceived on inspection. The NCAR array was set up in the field which had been mowed using standard agricultural machinery. The grass under the semi-permanent OKMN array had been cut with a hand operated device and the cut grass was left as straw on the surface.

Effect of shadowing. The shadowing of the viewed area under the radiometer arrays is also an issue. Although it could potentially cause an effective decrease of outgoing short-wave radiation flux, the calculations presented in the Appendix indicate that even at solar noon the effect is only $\sim 2\%$.

Sensor array level. Early in the deployment the response of the OKMN radiometers was somewhat skewed, indicating that the sensors were not completely level. On June 30 the problem was corrected and both the OKMN and NCAR responses became symmetrical about the solar noon maxima. It is noted that the response of the CNR1a to outgoing short-wave radiation is not symmetrical, but rather there is a deficit in the morning. This could be due to the location of the sensor on the support structure. However, as there is a suggestion of the same effect for the incoming short-wave radiation, it could be a more basic problem with the integrated CNR1 sensor.

Pyranometer nighttime response. The short-wave flux during the night is effectively zero. It is dark and the visible intensity, even under a full moon is five or six orders of magnitude less than at noon. $R_{\text{sw.in}}$ is $< 0.01 \text{ Wm}^{-2}$. However, the Eppley and the Kipp and Zonen pyranometers have negative instrumentation responses due to the real export of long-wave radiation by the devices. Immediately after sunset the effect is most intense, but the export persists throughout the night. Good ventilation reduces the problem. For Eppley pyranometers the response is $\sim -3 \text{ Wm}^{-2}$ and for the Kipp and Zonen CNR1 the response more serious with a value of $\sim -10 \text{ Wm}^{-2}$. The OKMN data system software sets any negative R_{sw} value to 0.0 Wm^{-2} . The ASTER system reports the spurious short-wave flux in order to monitor the effectiveness of the ventilation. The instrumentation response is only apparent at night but persists during the daytime.

Midday anomaly of up-looking pyrgeometers. An examination of the OASIS98 data indicated that the OKMN $lw.in$ persistently showed an anomalously elevated value for a few hours about solar noon. The reason for this effect was clearly revealed by the radiometer intercomparisons made at the end of the program. During the final day intercomparison, the two NCAR, the two OKMN and the CNR1, up-looking pyrgeometer responses were compared. During most of the diurnal cycle the traces of the four Eppley radiometers were quite similar, while the CNR1a showed a distinct $\sim +25 \text{ Wm}^{-2}$ offset. However, for the

several hour period around solar noon the responses of the different pyrgometers seriously diverged. lw.out NCAR had had a new dome installed immediately prior to OASIS98 and served as a reference. lw.in NCAR leaked $\sim 7 \text{ W m}^{-2}$ of short wave energy, (robust=F already invokes a 3.6% sw correction) lw.in OKMN leaked $\sim 18 \text{ W m}^{-2}$ of short wave energy lw.out OKMN leaked $\sim 40 \text{ W m}^{-2}$ of short wave energy

The presumption is that the silicon vacuum deposited coating on the inside of the pyranometer domes degrade over time when subjected to solar ultraviolet. The new dome on lw.out NCAR had not been previously exposed and was in the best condition. The other pyrgometers' domes were more degraded. The short wave leakage is not detected during the long-wave calibration of the sensor, as the calibration is carried out by exposing the pyrgometer to a black-body cavity maintained at different temperature. The black body cavity is completely dark in the shortwave spectral region. The effect operates only at high angles of shortwave illuminance and any correction must take this into account. A correction involving Rsw and the illuminance angle should be devised.

Positive offset of Kipp and Zonen CNR1 pyrgometer response. A discrepancy exists between the responses of the Kipp and Zonen CNR1 and the Eppley pyrgometers. The Kipp and Zonen CNR1 sensor persistently reports values some $+25 \text{ W m}^{-2}$ greater than for the two Eppley sensors, which are generally in agreement to within $\pm 5 \text{ W m}^{-2}$. This discrepancy increases by an extra 40 W m^{-2} for the midday period. The additional midday enhancement could be due to the uncorrected dome heating effect which, because the CNR1 long-wave radiometers lack the means to measure the dome temperature, is not applied. However, this cannot account for the persistent twenty four hour enhancement. The effect is best seen in the x:y scatter plots where it is apparent as an offset rather than a difference in gain or sensitivity. As $+25 \text{ W m}^{-2}$ corresponds to $\sim 5^\circ \text{ C}$ it is hard to imagine that this discrepancy is due to an error in the black body calibration of the Eppley pyrgometers.

ASTER algorithm. The treatment of the output from the different sensors is described earlier in this report. For the Eppleys the expression:

$$R_{lw} = R_{pile} + (1 + B) * SB * T_{case}^4 - B * SB * T_{dome}^4 - 0.035 R_{sw} \quad (1)$$

is used to calculate the long-wave radiation flux, with $B = 2.5$ for the correction due to pyrgometer dome opacity and 3.5% for the correction due to pyrgometer dome shortwave transparency. As we have discussed a simple constant value of 3.5% for this coefficient is no longer regarded as sufficient.

For the Kipp and Zonens the form of the calculation is not known. see ~/deployments/oasis/radioms.fm, oasis.q, okmn.q and deriv.q

Net radiation. For considerations of energy balance, the final product, the bottom line as it were, for the radiometers is the goodness of the net radiation flux. Table 7 shows the "error" for the various radiometers systems when compared to the NCAR four-component radiometer array

TABLE 7 Response difference from the NCAR four component array

Radiometer	Night-time ($- 50 \text{ W m}^{-2}$)		Noon ($+ 625 \text{ W m}^{-2}$)	
	OKMNsum	10 W m^{-2}	20%	25 W m^{-2} (anomaly removed)
NCARQ7	10 W m^{-2}	20%	15 W m^{-2}	2.5%
OKMNQ7	25 W m^{-2}	50%	20 W m^{-2}	3.2%
CNR1asum:	0 W m^{-2}	0%	30 W m^{-2}	4.8%
NRLite:	15 W m^{-2}	30%	50 W m^{-2}	8.0%

Appendix

Radiometer shadow

(These calculations were performed by Tom Horst. They indicate that the influence of the dark shadow as only of order ~2% of Rsw.out, even at midday when the influence of the shadow is at its maximum. As Rsw.out, at midday, has a value of 160 Wm^{-2} , the influence of the shadow is $\sim 3 \text{ Wm}^{-2}$, which is negligible)

The relative influence of a patch of surface dA to the up-welling radiation measurements is:

$$\begin{aligned} (dA/\pi) \cdot \cos(\theta)^2 / (z^2 + r^2)^2 &= \\ (dA/\pi) \cdot z^2 / (z^2 + r^2)^2 &= \\ dA / (\pi \cdot z^2) \cdot \cos(\theta)^4 & \end{aligned}$$

where:

z is the height of the radiometer,

r is the (horizontal) radial distance from the radiometer to the location dA,

theta is the nadir angle of dA from the radiometer.

This relationship is used to estimate the influence of the sawhorse shadow on the radiation measurements.

The integrated influence of a circular area of radius r_0 below the radiometer is $1/[1 + (z/r_0)^2]$, thus:

50% of the measurement is influenced by an area of radius $r_0 = z$,

80% of the measurement is influenced by an area of radius $r_0 = 2z$,

90% of the measurement is influenced by an area of radius $r_0 = 3z$,

96% of the measurement is influenced by an area of radius $r_0 = 5z$,

99% of the measurement is influenced by an area of radius $r_0 = 10z$.

Assuming that the Campbell box casts a circular shadow of radius $r_0 = 25\text{cm}$ directly below a radiometer at a height of 200cm , its influence is 0.015.

The area of a shadow with a width = w and a length = L centered below a radiometer at height = h has an influence equal to:

$$\begin{aligned} w/(\pi \cdot h) \cdot \{ (L/2h) / [1 + (L/2h)^2] + \text{atan}(L/2h) \} &= 0.02 \\ \text{for } w=10\text{cm, } h=200\text{cm, } L=400\text{cm} & \end{aligned}$$

Pyrgometer response

The equivalence of the two expressions given earlier for the NCAR algorithm is shown:

$$R_{aw} = R_{pile} + (1 + B) \cdot SB \cdot T_{case}^4 - B \cdot SB \cdot T_{dome}^4 - 0.035 R_{sw}$$

$$R_{lw} = R_{pile} + SB \cdot T_{case}^4 + B \cdot SB \cdot T_{case}^4 - B \cdot SB \cdot T_{dome}^4 - 0.035 R_{sw}$$

$$R_{lw} = R_{pile} + SB \cdot T_{case}^4 + B \cdot SB \cdot (T_{case}^4 - T_{dome}^4) - 0.035 R_{sw}$$

$$R_{lw} = R_{pile} + SB \cdot T_{case}^4 - B \cdot SB \cdot (T_{dome}^4 - T_{case}^4) - 0.035 R_{sw}$$

Tony Delany

delany/deployments/oasis/radioms.fm

OASIS98 figures

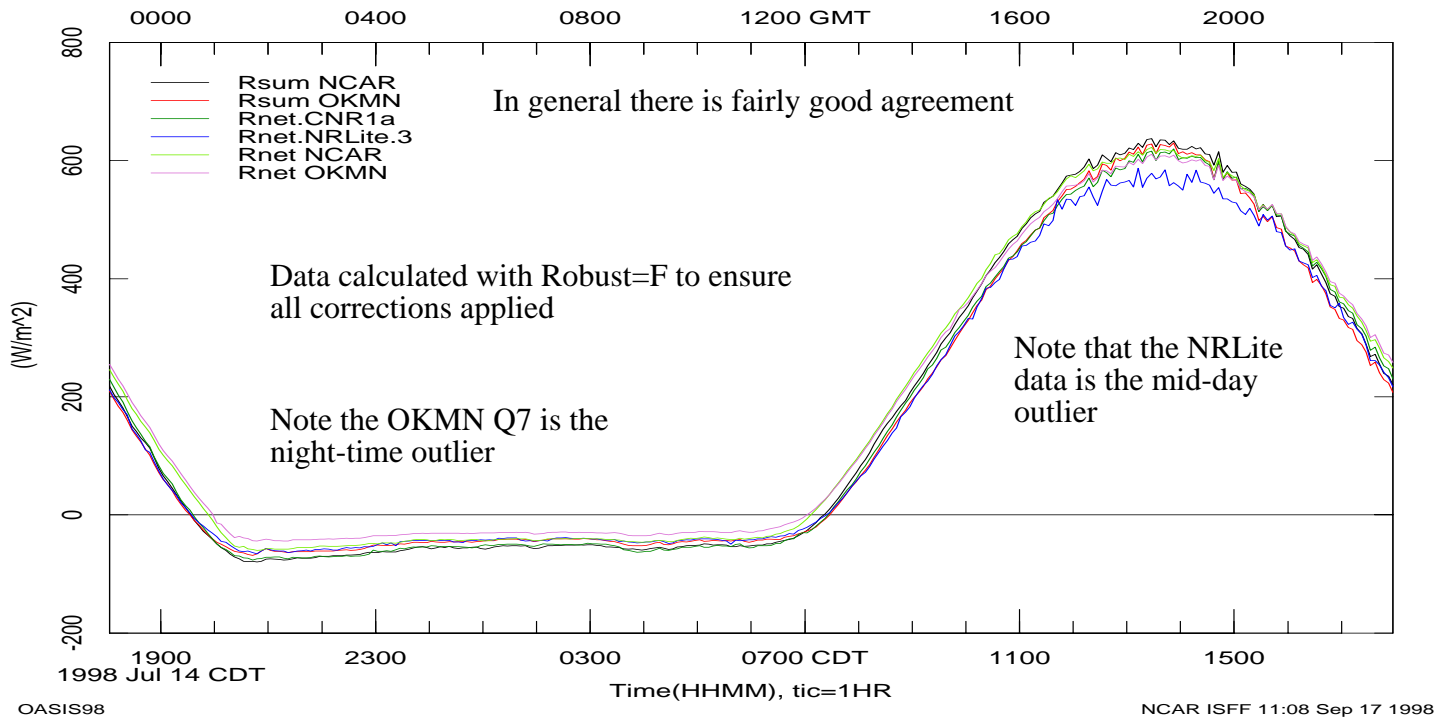


Figure 1. The sum and the net data for a good cloud-free day. There is fairly good agreement overall, although the NRLite and the OKMN Q7 sensors generate outlying data for mid-day and night-time, respectively.

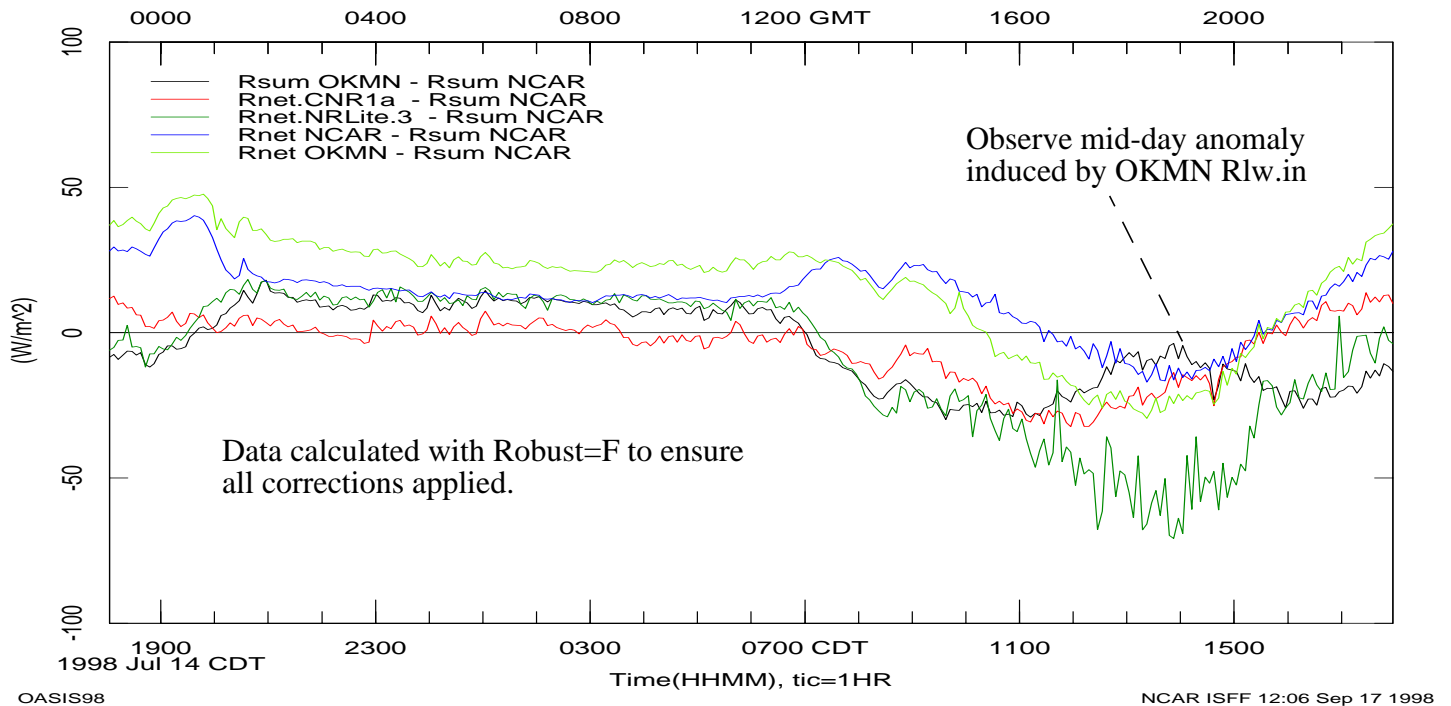


Figure 2. The sum and the net data for the same day plotted with reference to the difference to the sum of the NCAR four-component data. The mid-day spurious response of the OKMN up-looking pyrgeometer is apparent.

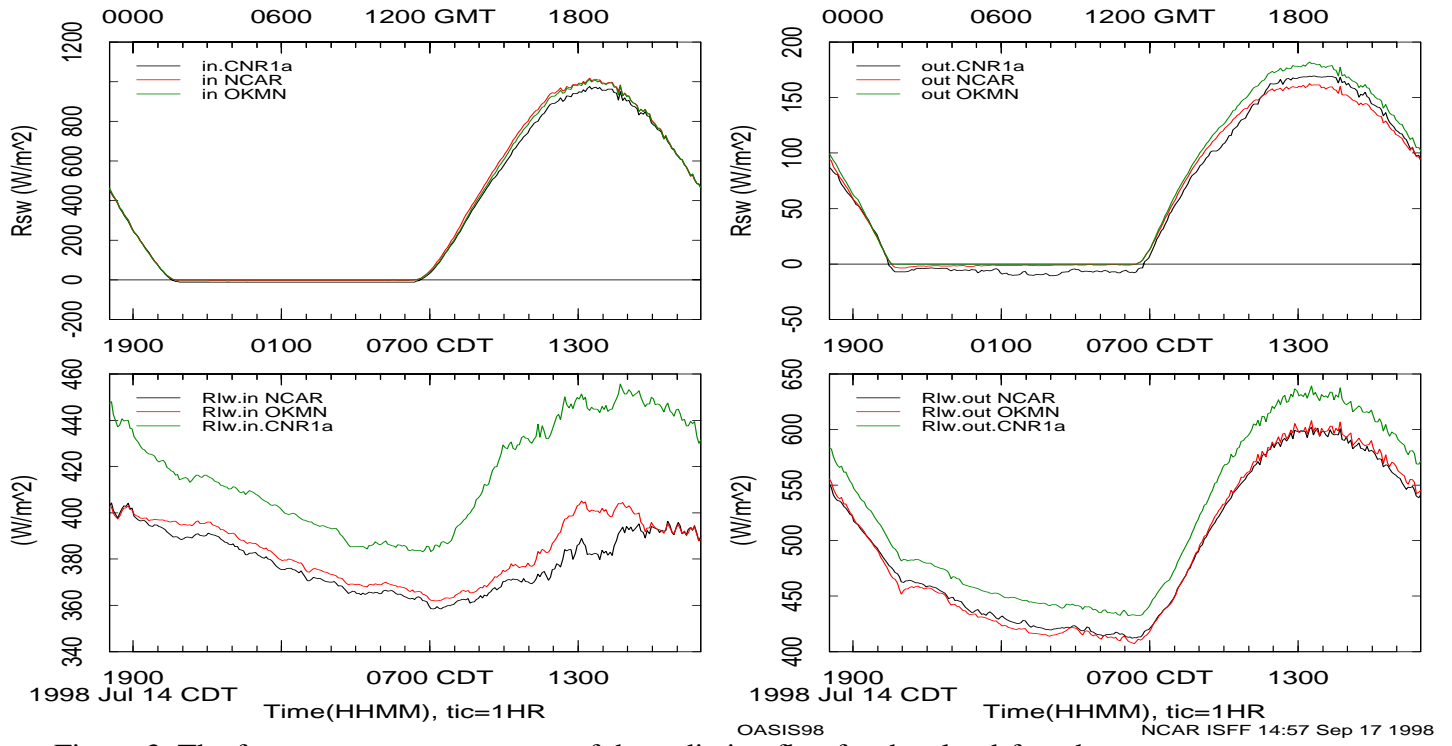


Figure 3. The four separate components of the radiation flux for the cloud-free day.

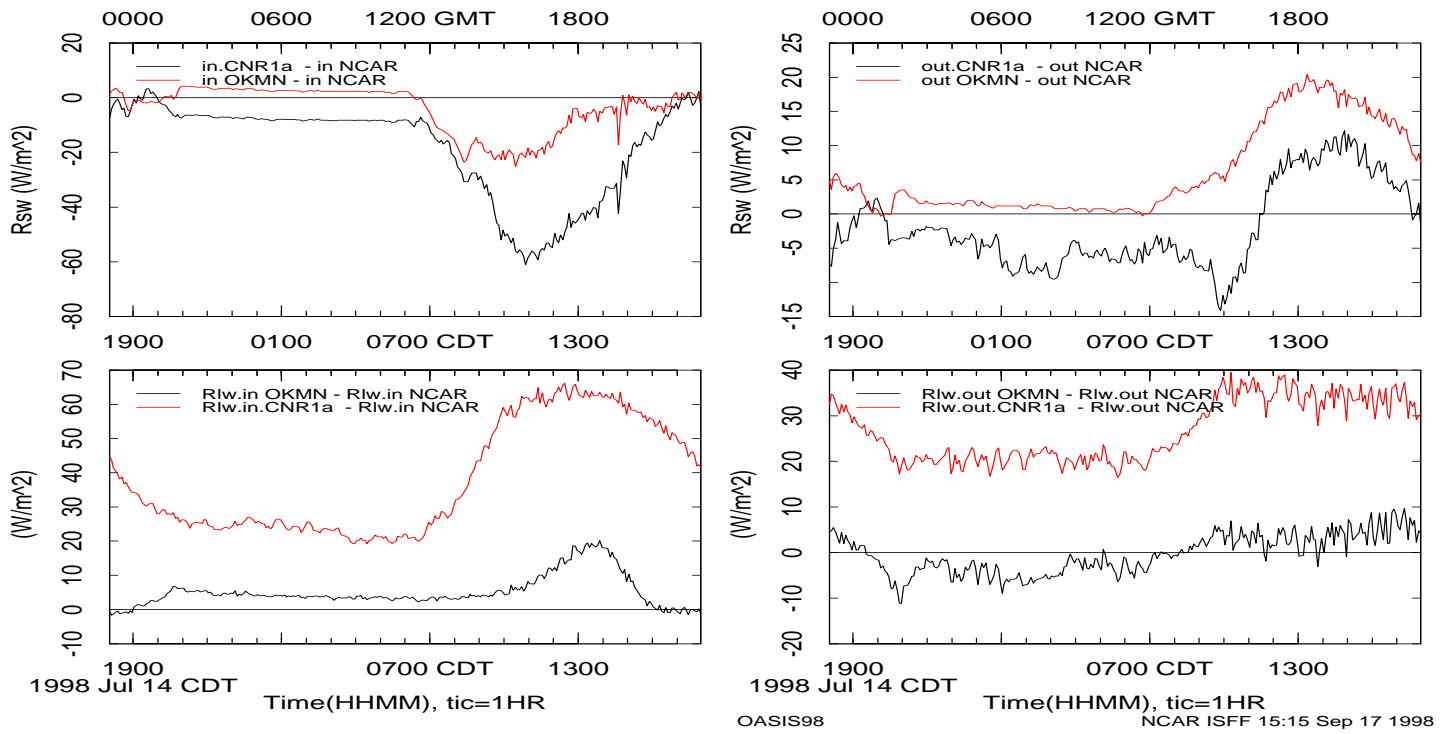
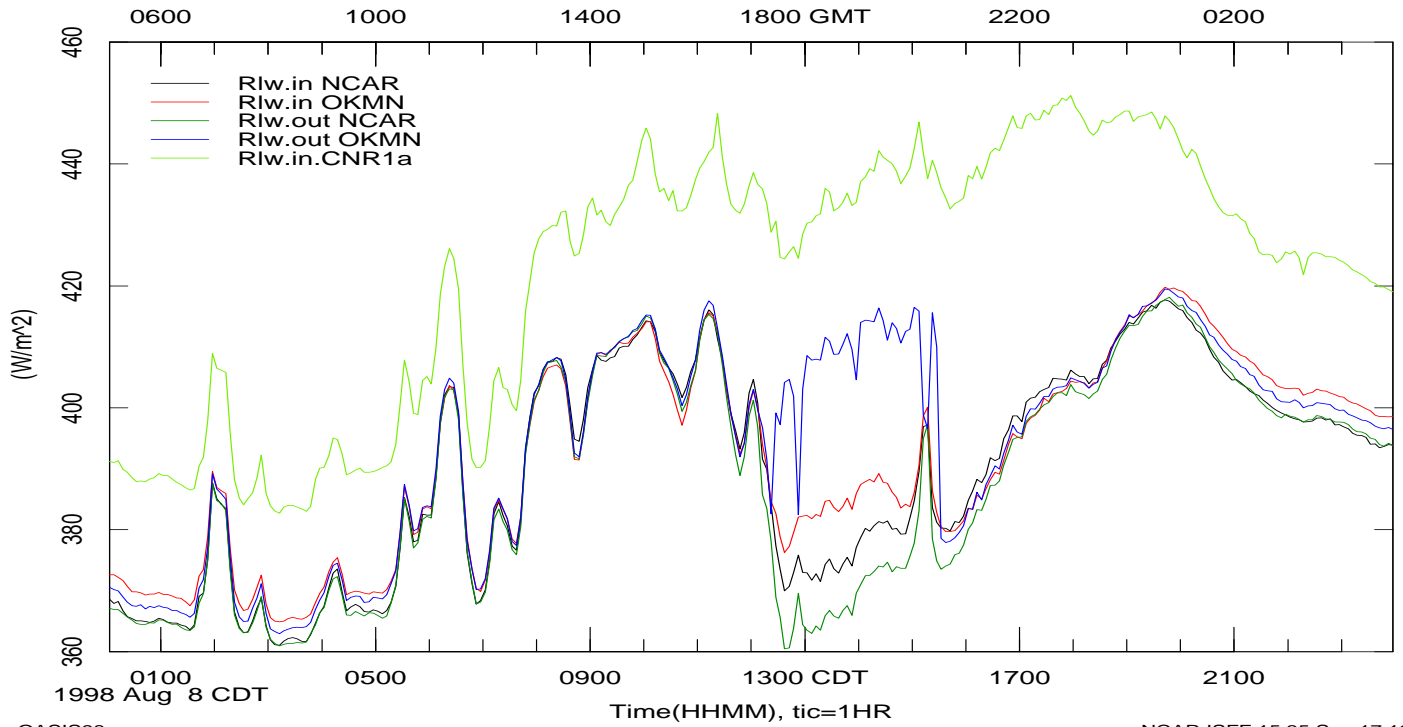


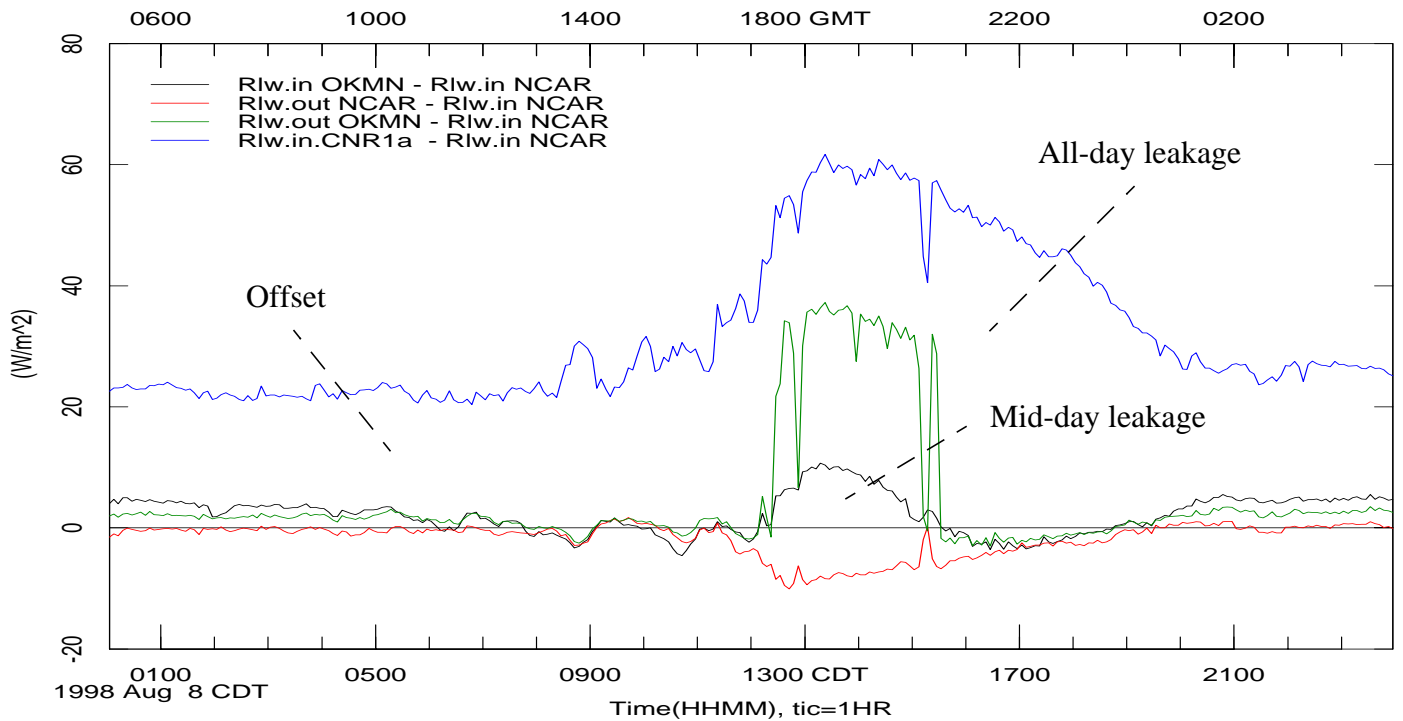
Figure 4. The differences of the four components from the NCAR Eppley system values. Note that for the incoming long-wave both the pyrgeometers exhibit apparent short-wave leakage.



OASIS98

NCAR ISFF 15:35 Sep 17 1998

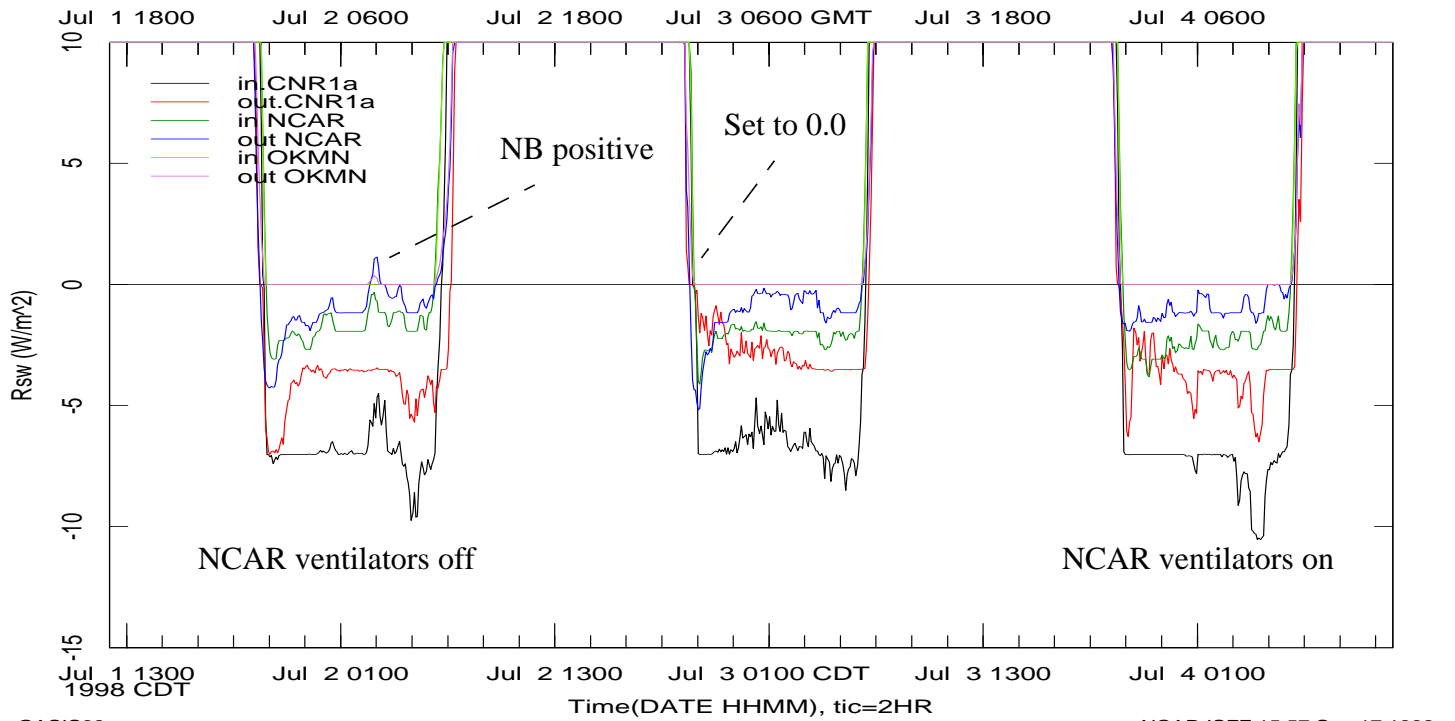
Figure 5. The effect of leakage of short-wave radiation through the pyrgemeter domes is shown. The problem is most severe in the mid-day. The full diurnal offset of the CNR1 pyrgemeter is most likely due to an error associated with the bad calculation of the sensor internal temperature



OASIS98

NCAR ISFF 15:43 Sep 17 1998

Figure 6. The short-wave leakage is illustrated better when the difference of response to the NCAR normally down-looking pyrgemeter is used as a reference. This sensor had had its dome replaced immediately prior to the OASIS98 deployment, and so had suffered no photodegradation.



OASIS98

NCAR ISFF 15:57 Sep 17 1998

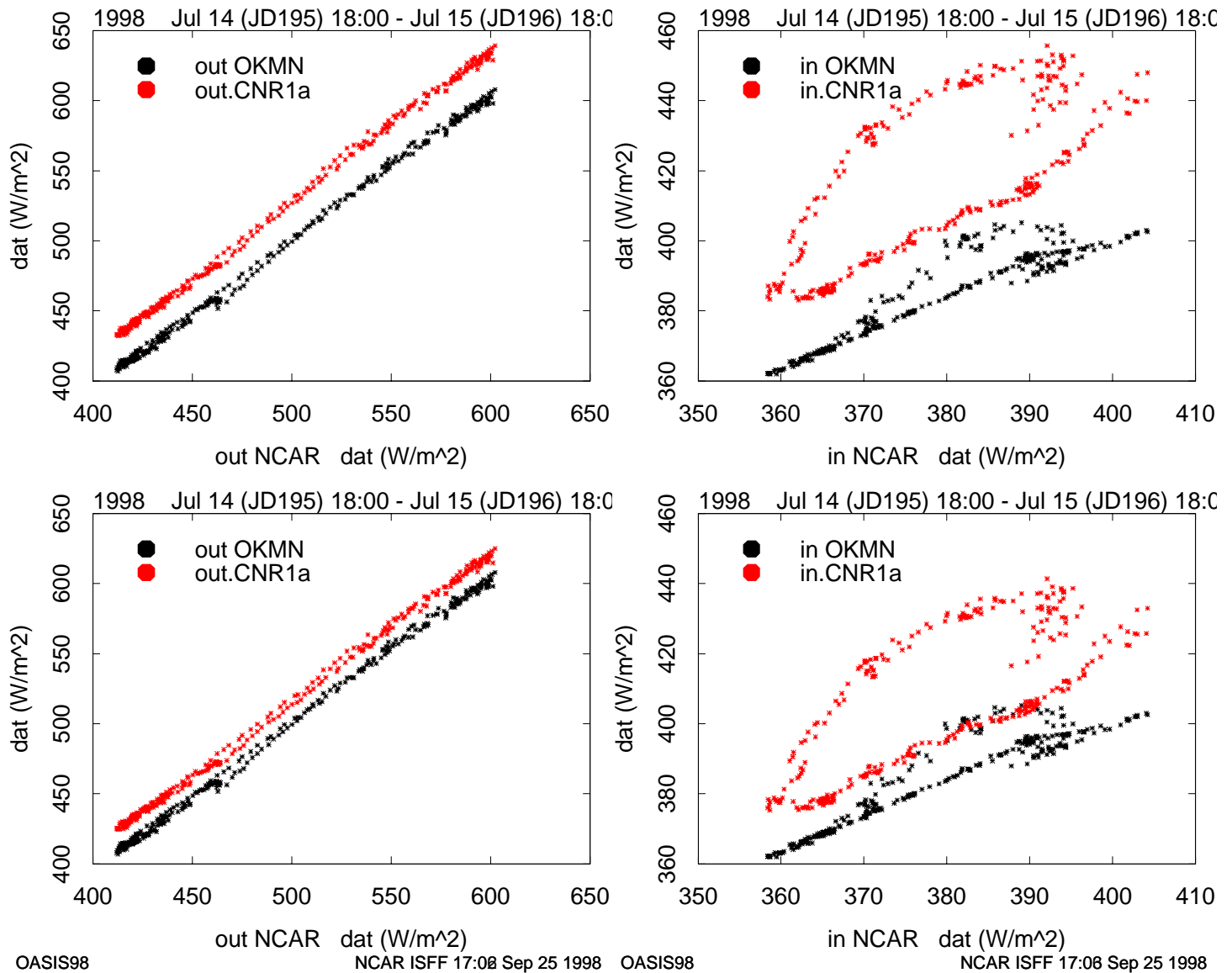
Figure 7. The night-time response of the various pyranometers. This response is an instrumentation effect. The pyranometers really do export radiation flux at night, especially just after sunset. They export long-wave radiation but the sensor system reports the flux as a “short-wave” flux. Note how better ventilation reduces the problem. The OKMN pyranometer outputs are set to 0.0 if they generate negative values. This is a legitimate tactic, but one which obscures the issue. Presumably the radiometers also function this way in the daytime.

Correction of the CNR1a data

The Kipp & Zonen integrated four component CNR1 radiometer utilizes a single internal temperature sensor to allow the compensation correction for both the incoming and the outgoing long-wave radiometers. During the OASIS98 program an incorrect calibration factor was operative. The result of using this incorrect calibration factor was recognized and an attempt was made to provide a better calibration factor.

The second calibration factor was applied to the data but it did not markedly improve the situation.

The top set of figures illustrate the CNR1a data with the original temperature calibration factor. The bottom set of figures illustrate the CNR1a data with the new temperature calibration factor.



Figures 8: using original temperature calibration factor for CNR1a.

Figures 9: using new temperature calibration factor for CNR1a.

Tony Delany
1999 April 19

/h/3/delany/deplymnets/oasis/radiation/radiomrep.fm